Modeling for Feedforward Control of Vehicle Velocity in Autonomous Bulldozers

Taro ABE[1]**, Genki Yamauchi**[1]**, Takeshi Hashimoto**[1]

[1] Public Works Research Institute, Japan

abe-t575co@pwri.go.jp, yamauchi-g573bs@pwri.go.jp, t-hashimoto@pwri.go.jp

Abstract -

In this paper, we propose a modeling approach for feedforward control of vehicle velocity in an autonomous bulldozer. Unlike tracked vehicles in which the left and right tracks can be commanded independently, a bulldozer is operated by two inputs-acceleration/deceleration and steering-analogous to throttle and steering-wheel inputs in passenger cars. Accordingly, the proposed method targets machines whose vehicle velocity is determined by two inputs. Specifically, a two-input forward model that maps the acceleration/deceleration and steering inputs to the translational and turning velocities is identified using vehicle velocity data measured on the actual machine. Then, the inverse mapping of the two-input forward model is solved numerically to convert a desired vehicle velocity input into the corresponding acceleration/deceleration and steering inputs accepted by the actual machine. Finally, we evaluated the error between the input vehicle velocity and the measured vehicle velocity when the input was applied using the proposed feedforward control. The results show that the proposed method enables vehicle velocity control within the range of vehicle velocities that the machine can produce.

Keywords -

Autonomous Bulldozer; Feedforward Control for Vehicle Velocity

1 Introduction

Construction sites face a growing labor shortage driven by population aging and a declining workforce. Reducing the required number of workers (labor savings) has therefore become a critical issue. As an effective means of labor savings, the use of automated construction machinery to substitute for tasks such as excavation and hauling, as well as automation across the entire construction process, has been actively pursued. To promote these efforts, the Public Works Research Institute (PWRI), Japan, has been developing OPERA (Open Platform for Earthwork with Robotics and Autonomy) [1].

1.1 OPERA

OPERA aims to accelerate research and development of autonomous construction by providing, as open resources, tools and technical information required for developing autonomous earthwork technologies, thereby lowering the barrier to entry not only for construction companies and heavy-machinery manufacturers but also for universities and software companies from other industries. OPERA provides autonomous-machine platforms, simulation environments, and common control signals that can be shared between actual machines and simulators. Within this framework, an autonomous bulldozer is being developed as one of the target platforms for automated earthwork operations.

1.2 Objective and contribution of this study

The objective of this study is to construct and validate a feedforward controller for an autonomous bulldozer that converts a desired vehicle velocity input, $\boldsymbol{x} = [v, \omega]^\top$, into the acceleration/deceleration and steering commands accepted by the actual machine. The contribution of this paper does not include simulation; rather, it focuses on the construction of the feedforward controller and experimental validation.

Unlike tracked vehicles in which the left and right tracks can be commanded independently, a bulldozer accepts traveling inputs only in the form of acceleration/deceleration and steering commands. Therefore, the generation of machine commands from a desired vehicle velocity must be treated as an inverse problem of a coupled two-input mapping. In this paper, we identify a two-input forward model from measurements on the actual machine, numerically solve its inverse mapping, and evaluate the resulting feedforward controller through experiments on the actual bulldozer.

2 Related Work

For tracked vehicles such as hydraulic excavators, if independent inputs can be applied to the left and right tracks, a desired vehicle velocity input (v, ω) can be kinematically decomposed into target track speeds, and actual machine inputs can then be generated via the inverse mappings of the identified input–speed characteristics for each track. As a representative example, Frese *et al.* [2] proposed feedforward control by identifying the relationship between track motion inputs and track speeds and then using its inverse mapping, combined with correction based on velocity error, to achieve locomotion control.

In contrast, for bulldozers, the accepted traveling inputs are not independent inputs for each track but are provided as acceleration/deceleration and steering inputs. Therefore, although decomposing (v, ω) into left and right track speeds is possible, the final generation of actual machine inputs cannot be separated per track and must be treated as an inverse problem of a two-input mapping [3, 4]. The next section formulates the inverse problem for two-input systems and presents a method for feedforward control.

3 Feedforward Control of Vehicle Velocity

3.1 General Form of Feedforward Control of Vehicle Velocity

A conversion model that generates lever/button-level control inputs $\boldsymbol{u} \in \mathbb{R}^i$ from a vehicle velocity input $\boldsymbol{x} \in \mathbb{R}^k$ is expressed as

$$\boldsymbol{u} = \boldsymbol{F}_u(\boldsymbol{x}). \tag{1}$$

Here, "lever/button-level control inputs" denote inputs equivalent to an operator's lever/button actions (steering and acceleration/deceleration) and accepted by the actual machine. The dimension k denotes the dimension of the vehicle velocity input; for example, $k = 2$ for translational velocity v and turning velocity ω. Similarly, i denotes the dimension of the lever/button-level control inputs. For tracked vehicles in which the left and right tracks can be driven by independently specified inputs, $i = 2$ and $\boldsymbol{u} = [u_1, \dots, u_i]^\top$ can represent the left/right track-speed inputs.

A forward model of the vehicle velocity $\boldsymbol{x}$ observed for given inputs $\boldsymbol{u}$ is written as

$$\boldsymbol{x} = \boldsymbol{G}(\boldsymbol{u}). \tag{2}$$

If the forward model $\boldsymbol{G}$ can be identified, then finding $\boldsymbol{u}$ corresponding to a desired vehicle velocity input $\boldsymbol{x}$ can be formulated as an inverse mapping problem:

$$\boldsymbol{u} = \boldsymbol{G}^{-1}(\boldsymbol{x}). \tag{3}$$

3.2 Feedforward Control of Vehicle Velocity in a Bulldozer

Figure 1 outlines the feedforward control for vehicle velocity in a bulldozer. Given a vehicle velocity input $\boldsymbol{x} = [v, \omega]^\top$, the feedforward control outputs the acceleration/deceleration and steering inputs $\boldsymbol{u} = [d, t]^\top$ as

$$\boldsymbol{u} = \boldsymbol{F}_u(\boldsymbol{x}; s), \tag{4}$$

where d denotes the acceleration/deceleration input and t denotes the steering input accepted by the actual machine. The discrete variable $s \in \{\mathrm{F}, \mathrm{R}\}$ indicates forward/reverse selection. In practice, reverse motion ($s = \mathrm{R}$) can be handled by sign inversion of the translational velocity with respect to the forward model ($s = \mathrm{F}$), allowing the problem to be treated as solving only for $\boldsymbol{u} = [d, t]^\top$ under $s = \mathrm{F}$. The implementation procedure of the feedforward control for a bulldozer is described below.

Identification of the forward model. This paper models the forward relationship between the acceleration/deceleration and steering inputs $\boldsymbol{u} = [d, t]^\top$ and the vehicle velocity $\boldsymbol{x} = [v, \omega]^\top$ measured on the actual machine, i.e., the forward model $\boldsymbol{x} = \boldsymbol{G}(\boldsymbol{u})$. During data acquisition, $\boldsymbol{u}$ is applied and the resulting vehicle velocity is measured, yielding input–output pairs $(\boldsymbol{u}, \boldsymbol{x})$ for identifying $\boldsymbol{G}$.

Feedforward control as an inverse mapping. For the identified forward model $\boldsymbol{G}$, the acceleration/deceleration and steering inputs consistent with a desired vehicle velocity input $\boldsymbol{x} = [v, \omega]^\top$ are obtained by solving an inverse problem that searches for $\boldsymbol{u}$ satisfying $\boldsymbol{G}(\boldsymbol{u}) \approx \boldsymbol{x}$. Because the inputs are subject to constraints such as lower and upper bounds, the mapping is defined as

$$\begin{aligned}\boldsymbol{u}(\boldsymbol{x}) = \begin{bmatrix} d(\boldsymbol{x}) \\ t(\boldsymbol{x}) \end{bmatrix} &= \begin{bmatrix} F_d(v, \omega; s) \\ F_t(v, \omega; s) \end{bmatrix} \\ &= \arg \min_{\boldsymbol{u}=[d,t]^\top \in \mathcal{U}} \|\boldsymbol{G}(\boldsymbol{u}) - \boldsymbol{x}\|_2^2,\end{aligned} \tag{5}$$

where $\mathcal{U}$ denotes the feasible set of acceleration/deceleration and steering inputs. Accordingly, $\boldsymbol{F}_u(\boldsymbol{x}; s)$ is implemented as a mapping that simultaneously solves for d and t by numerically solving the inverse of the forward model $\boldsymbol{G}$. Because a closed-form derivation of this mapping is difficult, this paper derives it using a Newton-type method described in the next subsection.

3.3 Bounded inverse mapping from vehicle velocity input $\boldsymbol{x}$ to acceleration/deceleration and steering inputs $\boldsymbol{u}$

This subsection describes a bounded inverse mapping used to convert a target vehicle velocity input $\boldsymbol{x}^* = [v^*,\ \omega^*]^\top$ into the acceleration/deceleration and steering inputs $\boldsymbol{u} = [d,\ t]^\top$, where d denotes the acceleration/deceleration input and t denotes the steering input accepted by the actual machine.

Forward model. A forward model is identified beforehand to represent the relationship between the acceleration/deceleration and steering inputs $\boldsymbol{u} = [d,\ t]^\top$ and the resulting vehicle velocity:

$$\boldsymbol{G}(\boldsymbol{u}) := \begin{bmatrix} v_{\text{out}}(d, t) \\ \omega_{\text{out}}(d, t) \end{bmatrix}. \tag{6}$$

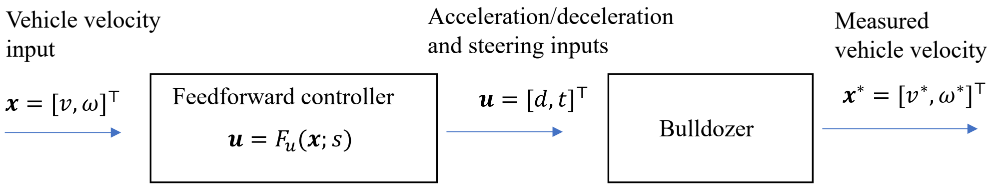

Figure 1. Overview of the feedforward control of vehicle velocity in a bulldozer

Bounding transform. Since the acceleration/deceleration and steering inputs must satisfy the physical bounds $d \in [d_{\min}, d_{\max}]$ and $t \in [t_{\min}, t_{\max}]$, we introduce an unconstrained variable $\boldsymbol{z} = [z_d,\ z_t]^\top \in \mathbb{R}^2$ and a logistic bounding transform $\boldsymbol{\sigma}(\cdot)$:

$$\boldsymbol{u} = \boldsymbol{\sigma}(\boldsymbol{z}) = \begin{bmatrix} \sigma_d(z_d) \\ \sigma_t(z_t) \end{bmatrix}, \tag{7}$$

$$\begin{aligned} \sigma_d(z_d) &= d_{\min} + \frac{d_{\max} - d_{\min}}{1 + e^{-z_d}} \\ \sigma_t(z_t) &= t_{\min} + \frac{t_{\max} - t_{\min}}{1 + e^{-z_t}}. \end{aligned} \tag{8}$$

This formulation guarantees that any $\boldsymbol{z} \in \mathbb{R}^2$ always yields bounded acceleration/deceleration and steering inputs $\boldsymbol{u}$ within the allowable ranges, avoiding divergence to infeasible values during numerical iterations.

Inverse solution by root finding. The inverse problem is formulated as solving a two-dimensional root-finding problem in $\boldsymbol{z}$:

$$\boldsymbol{F}(\boldsymbol{z}) := \boldsymbol{G}(\boldsymbol{\sigma}(\boldsymbol{z})) - \boldsymbol{x}^*, \qquad \text{find } \hat{\boldsymbol{z}} \text{ such that } \boldsymbol{F}(\hat{\boldsymbol{z}}) = \boldsymbol{0}. \tag{9}$$

In our implementation, $\hat{\boldsymbol{z}}$ is computed using a Newton-type iterative method. After convergence, the bounded inputs are obtained by restoring the variables through the same transform:

$$\hat{\boldsymbol{u}} = \boldsymbol{\sigma}(\hat{\boldsymbol{z}}) = \begin{bmatrix} \hat{d} \\ \hat{t} \end{bmatrix}, \qquad \boldsymbol{r} = \boldsymbol{F}(\hat{\boldsymbol{z}}), \tag{10}$$

where $\boldsymbol{r}$ denotes the residual vector used to evaluate the solution quality.

4 Experimental Setup

This section describes the experimental setup for modeling the feedforward control and evaluating the accuracy of the feedforward control.

4.1 System configuration of the autonomous bulldozer in OPERA

Figure 2 shows the system configuration of the autonomous bulldozer used in this study. The base machine is a bulldozer D37PXi (Komatsu Ltd.), and the system enables bulldozer control by electrically overriding the signals corresponding to the vehicle's operator inputs. This electrical intervention is implemented via an external ECU (Electronic Control Unit) developed for this study. The acceleration/deceleration and steering inputs generated by an external computer (e.g., a PC) are output as CAN signals, converted into analog signals by the external ECU, and then transmitted to the vehicle's electrical system. The overridden signals include those for crawler control, blade control, and the control switches of the onboard semi-automatic blade system (In Japan, it is called "MC (machine control)"), such as the enable/disable switch and the cut-and-fill height adjustment switch.

To obtain the vehicle's self-position and heading (yaw angle), a GNSS compass V500 (Hemisphere GNSS, Inc.) is installed. Positioning information from the GNSS compass is sent to the external computer via serial communication. In addition, IMU G2 (Novatron) is installed on both the vehicle body and the blade to measure their attitudes, and the measured attitude information is transmitted to the external computer via CAN.

The autonomous bulldozer supports not only operation by the external computer but also teleoperation by an operator. Specifically, wireless signals transmitted from a teleoperation device are relayed to the external ECU via a receiver to realize teleoperation.

For visualization of the machine state, the external ECU controls a signal light to make the operating state externally visible. A wireless emergency stop device is also installed to safely stop the machine in an emergency.

4.2 Observation of vehicle velocity $\boldsymbol{x} = [v, \omega]^\top$

To identify the forward model $\boldsymbol{x} = \boldsymbol{G}(\boldsymbol{u})$, the translational velocity v and turning velocity ω of the vehicle are measured in response to acceleration/deceleration and steering inputs. For measuring translational and turning velocities, we use the self-position and attitude (yaw angle) information obtained from the GNSS compass. Specifically, the bulldozer is driven over a fixed segment (or for a fixed duration), and the velocity is computed by numerically differentiating (finite differencing) the time-series data of position and yaw angle. The time-averaged values over the driving segment are then used as (v, ω). To

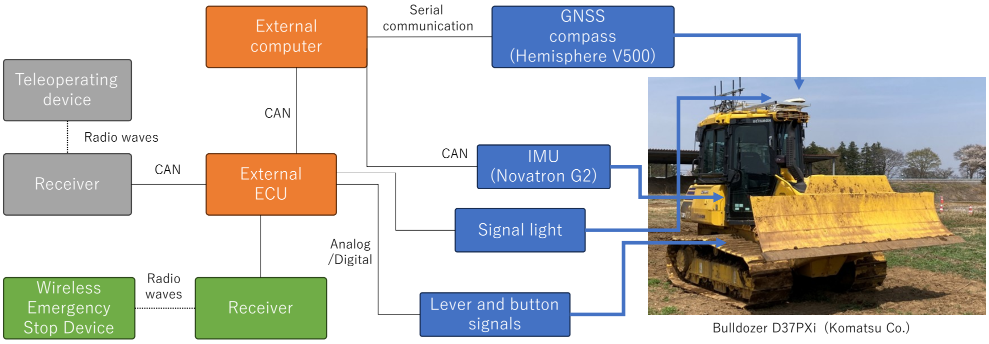

Figure 2. System overview of the autonomous bulldozer in OPERA.

reduce the effect of measurement noise introduced by numerical differentiation, temporal averaging and smoothing are applied over the driving segment.

4.3 Experimental conditions

Setting the maximum track surface speed. The bulldozer used in this study allows selection of a gear (shift) setting depending on the application, similar to shift operation in passenger cars, and differences in the gear setting affect the vehicle-velocity characteristics for the same acceleration/deceleration and steering inputs. Therefore, this paper explicitly specifies the gear setting as an experimental condition. The machine provides both a mode that allows continuous speed-range changes and a mode that switches discretely among first, second, and third gears; this paper uses the latter.

In OPERA, the autonomous bulldozer is being developed primarily to automate dozing operations in earthwork. In such operations, the bulldozer mainly pushes soil that has been dumped by crawler dump trucks. Based on interviews with bulldozer operators, first gear is typically selected for dozing operations with the D37PXi (among the first to third gears); therefore, the experiments in this paper set the traveling speed range to first gear. In this condition, the maximum track surface speed is approximately 0.94 m/s.

Data acquisition site. The data acquisition site is the PWRI DX Field, which consists of loam.

5 Experimental Results and Discussion 1: Modeling feedforward control of vehicle velocity

The parameters of the forward model $\boldsymbol{x} = \boldsymbol{G}(\boldsymbol{u})$ for vehicle velocity $\boldsymbol{x} = [v, \omega]^\top$ (v: translational velocity, ω: turning velocity) as a function of acceleration/deceleration and steering inputs $\boldsymbol{u} = [d, t]^\top$ (d: acceleration/deceleration input, t: steering input) are identified based on measured vehicle velocity data. Specifically, the model coefficients of $v_{\text{out}}(d, t)$ and $\omega_{\text{out}}(d, t)$ are estimated from paired data of the acceleration/deceleration and steering inputs $\boldsymbol{u} = [d, t]^\top$ and the measured vehicle velocity $\boldsymbol{x} = [v, \omega]^\top$.

Table 1. Input ranges of lever/button-level control inputs and corresponding machine behaviors

Variable	Input range	Behavior
d	$0 \sim 255$	0–80: maximum speed ≥ 162: vehicle stopped
t	$-126 \sim 127$	negative: left turn 0: straight positive: right turn
s	$\{0, 1, 2\}$	0: neutral 1: forward 2: reverse

5.1 Acquisition of vehicle velocity measurement data and identification of the forward model

By varying $\boldsymbol{u} = [d, t]^\top$ and measuring the corresponding $\boldsymbol{x} = [v, \omega]^\top$, we construct a dataset for identifying the forward model $\boldsymbol{x} = \boldsymbol{G}(\boldsymbol{u})$.

Definition of inputs. As described in Section 4, acceleration/deceleration and steering inputs are applied by converting lever/button-level control inputs into electrical signals. The input ranges representing the input magnitudes and the corresponding machine behaviors are summarized in Table 1.

Following Section 3, the forward/reverse selection is represented as $s \in \{\mathrm{F}, \mathrm{R}\}$. Because vehicle velocity measurements in this section are collected under forward motion, we set $s = 1$ (i.e., $s = \mathrm{F}$) during data acquisition. Accordingly, this section treats s as fixed, and identifies the forward model from sample data obtained by applying combinations of d and t.

Sample design. The combinations of sampled data points were determined by considering the preliminary observations with respect to the input range in preliminary operations, including saturation regions where the output plateaus near the upper input range and dead zones where the machine does not move. Specifically, we used d: 0, 80, 100, 120, 140, 162 and t: 0, 30, 60, 80, 100, 127, resulting in a total of $6 \times 6 = 36$ samples.

The sampled data points in Figures 3 and 4 are used as an identification dataset for constructing the nominal inverse mapping. Each point corresponds to a single trial under the corresponding input condition and is intended to capture the overall trend of the input-output relationship, rather than the statistical repeatability at each grid point.

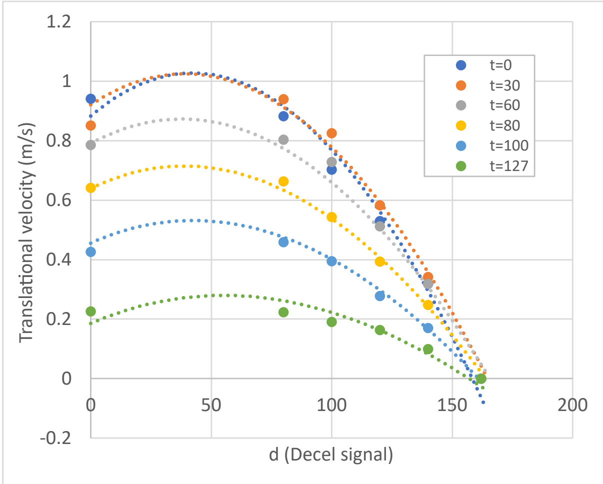

Figure 3. Distribution of translational velocity v when varying the acceleration/deceleration input d with fixed steering input t: points denote samples (pairs of translational and turning velocities), and dotted lines denote forward model fits for sample groups with fixed t.

Measurement results and discussion. Figure 3 shows the distribution of translational velocity v when varying d while keeping the steering input t fixed. The figure indicates that the output generally saturates when $d \leq 80$. It also shows a tendency for v to decrease as t increases. For all values of t, $v \simeq 0$ when $d = 162$.

Figure 4 shows the distribution of turning velocity ω when varying t while keeping the acceleration/deceleration input d fixed. The figure indicates that ω tends to increase as d decreases.

Although some samples deviate from the above trends, the primary cause is considered to be ground unevenness in the driving environment.

5.2 Forward model identification and discussion

From the observed trends, the outputs vary smoothly with respect to the inputs in general; therefore, the forward model is obtained using polynomial approximation. In this paper, $v_{\mathrm{out}}(d,t)$ and $\omega_{\mathrm{out}}(d,t)$ are expressed as bivariate third-order polynomials as follows, and the coefficients (A and B) are estimated using Wolfram Mathematica [5].

$$v_{\mathrm{out}}(d,t) = A_1\, d^3 + A_2\,(d^2\, t) + A_3\, d^2 + A_4\,(d\, t^2) + A_5\,(d\, t) + A_6\, d + A_7\, t^3 + A_8\, t^2 + A_9\, t + A_{10} \tag{11}$$

$$\omega_{\mathrm{out}}(d,t) = B_1\, d^3 + B_2\,(d^2\, t) + B_3\, d^2 + B_4\,(d\, t^2) + B_5\,(d\, t) + B_6\, d + B_7\, t^3 + B_8\, t^2 + B_9\, t + B_{10} \tag{12}$$

Table 2. Coefficient mapping for $v_{\mathrm{out}}(d,t)$

Coefficient	Value	Term
A_1	2.59353×10^{-8}	d^3
A_2	3.83565×10^{-7}	d^2t
A_3	-8.25610×10^{-5}	d^2
A_4	2.19745×10^{-7}	dt^2
A_5	-5.43348×10^{-5}	dt
A_6	6.84850×10^{-3}	d
A_7	3.46982×10^{-7}	t^3
A_8	-1.23878×10^{-4}	t^2
A_9	4.64519×10^{-3}	t
A_{10}	0.883125	constant

The estimated coefficients of the forward model are listed in Table 2 and Table 3.

In Figure 3 and Figure 4, the polynomial approximations are overlaid as dotted lines on the sample points (pairs of translational and turning velocities). The color of each dotted line matches the corresponding sample-point color: in Figure 3, the same-colored dotted line represents the forward model fit for the sample group with a fixed steering input t, while in Figure 4, it represents the fit for the sample group with a fixed acceleration/deceleration input d.

These distributions indicate that, for both translational and turning velocities, the fitted functions generally follow the samples in the range d = 80–160. In contrast, in the range d = 0–80, there exist regions where the polynomial approximation deviates from the measured values due to limitations of polynomial fitting. For this range, during numerical derivation of the inverse of the forward model, we adjust the convergence destination by selecting an appropriate initial value for the Newton iterations, and we do not use solutions corresponding to this region in the computation.

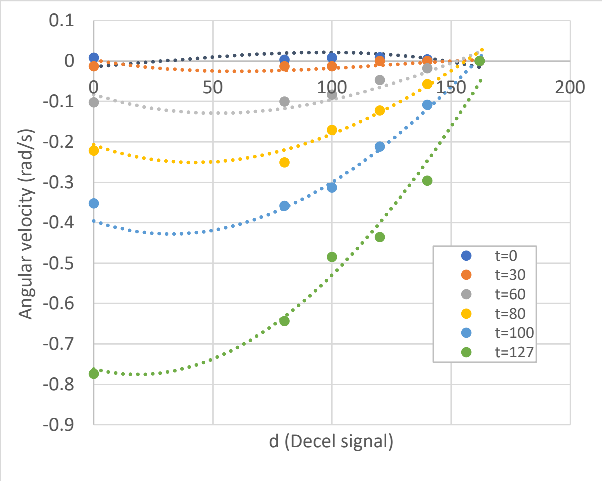

Figure 4. Distribution of turning velocity ω when varying the steering input t with fixed acceleration/deceleration input d: points denote samples (pairs of translational and turning velocities), and dotted lines denote forward model fits for sample groups with fixed d.

Table 3. Coefficient mapping for $\omega_{\text{out}}(d, t)$

Coefficient	Value	Term
B_1	-3.09580×10^{-8}	d^3
B_2	3.07046×10^{-7}	d^2t
B_3	2.25784×10^{-6}	d^2
B_4	3.52321×10^{-7}	dt^2
B_5	-5.99508×10^{-5}	dt
B_6	4.36811×10^{-4}	d
B_7	-1.46943×10^{-7}	t^3
B_8	-4.33994×10^{-5}	t^2
B_9	1.99288×10^{-3}	t
B_{10}	-1.38673×10^{-2}	constant

6 Experimental Results and Discussion 2: Evaluation of the proposed feedforward control

The accuracy of the feedforward control $\boldsymbol{u} = \boldsymbol{F}_u(\boldsymbol{x})$, obtained from the forward model identified in the previous section, is evaluated through experiments on the actual machine. Specifically, for a desired vehicle velocity input $\boldsymbol{x} = [v, \omega]^\top$, the generated acceleration/deceleration and steering inputs $\boldsymbol{u} = [d, t]^\top$ are applied to the vehicle and compared with the measured vehicle velocity.

Input definition. Vehicle velocity inputs $\boldsymbol{x} = [v, \omega]^\top$ were given, and the resulting translational and turning velocities were compared with the input values. For each sampled vehicle-velocity condition, the experiment was repeated three times.

To compare the errors in translational and turning velocities on a common scale, the normalized error ratios were calculated with respect to the maximum translational velocity and the maximum turning velocity, respectively. Specifically, the normalized error ratio of translational velocity E_v and that of turning velocity E_ω are defined as

$$E_v = \frac{v_{\text{out}} - v_{\text{in}}}{v_{\max}}, \tag{13}$$

$$E_\omega = \frac{\omega_{\text{out}} - \omega_{\text{in}}}{\omega_{\max}}, \tag{14}$$

where $v_{\max} = 0.94\,\text{m/s}$ is the maximum translational velocity and $\omega_{\max} = 0.74\,\text{rad/s}$ is the maximum turning velocity considered in this study.

Results and discussion. The distributions of the measured vehicle velocities for the vehicle velocity input $\boldsymbol{x}$ are shown in Figure 6 and Figure 7. Each figure represents the mean of the three trials. To make the remaining error and dispersion explicit about the measured values relative to the input, Figures 8 and 9 additionally show the normalized error ratio with respect to the maximum translational velocity and the maximum turning velocity considered in the evaluation.

For translational velocity, the error becomes relatively large when the input is close to 0.0 m/s, whereas under the other operating conditions, the error remains within an approximately limited range of ±10%. The reason the error becomes relatively large around an input translational velocity of 0.0 m/s is that the samples where the error rate exceeded 10% at a translational velocity of 0.0 m/s were recorded during the bulldozer's in-place turn. In such cases, it is possible that the center of rotation of the machine on the ground did not coincide with the geometric center of gravity of the vehicle. Therefore, even if the true translational velocity was 0.0 m/s, it is thought that the translational velocity was observed due to this discrepancy.

For turning velocity, both the error and the trial-to-trial dispersion tend to increase as the target turning velocity becomes larger, and this tendency is particularly visible in the range of approximately 0.3 to 0.6 rad/s. One possible reason for this is that there is a limit to the torque that a crawler can output. At relatively low turning velocities, there is sufficient torque margin (The difference between the maximum torque and the current torque) to realize the commanded motion, and the influence of small changes in the ground condition is limited. In contrast, at higher turning velocities, the torque required to achieve the target motion increases and the available torque margin becomes smaller. As a result, the turning response will become more sensitive to slight changes in the ground condition and slip, and the actual turning velocity tends to fluctuate.

Overall, this evaluation indicates that the errors in rotational velocity tend to be larger than those in translational

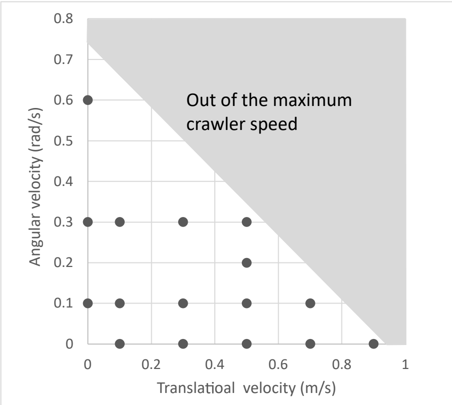

Figure 5. Sample distribution of vehicle velocity inputs $\boldsymbol{x} = [v, \omega]^\top$ for evaluating the feedforward control

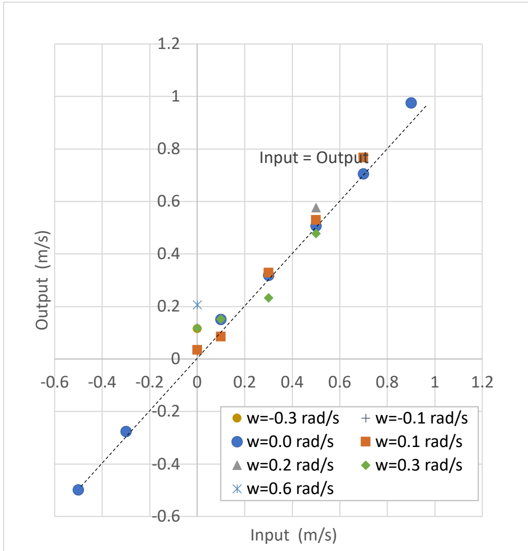

Figure 6. Measured translational velocity for the vehicle velocity input $\boldsymbol{x}$

velocity. A possible explanation is that crawler-type vehicles generate slip against the ground while turning, making their motion more sensitive to the effects of ground contact and friction. In addition to the factors discussed above, the observed dispersion may also be influenced, under some conditions, by the convergence of the inverse mapping to a local solution. A detailed analysis of this effect remains as future work.

7 Conclusion

This paper addressed the construction and validation of a feedforward controller for an autonomous bulldozer based on an inverse mapping from a desired vehicle velocity input, $\boldsymbol{x} = [v, \omega]^\top$, to the acceleration/deceleration and steering inputs accepted by the actual machine. To achieve this objective, we identified a two-input forward model from measured data on the actual bulldozer, and then numerically solved its inverse to generate the corresponding lever-level traveling inputs. The proposed method was evaluated through experiments on the actual machine, and the results confirmed that the target trend of translational and turning velocities can be reproduced within the range of vehicle velocities achievable by the machine.

Limitations. Although the proposed method reproduced the vehicle velocity within the achievable operating range, repeated measurements were not conducted for all identification points used to construct the map in Figures 3 and 4. Therefore, additional data acquisition is required to further improve the reliability of the map itself. In addition, the present experiments were performed under a no-load condition, namely without soil or other material accumulated on the blade, and the validity of the proposed method under loaded operating conditions has not yet been verified.

Future work. As future work, the amount of data used for the map generation should be increased, and repeated measurements should be conducted for each input condition so that the inverse mapping can be constructed using averaged responses rather than single-trial values.

In addition, vehicle velocity control that accounts for changes in vehicle behavior due to load variations during dozing operations and during traversal over uneven terrain is required. During dozing, even if feedforward control is applied with the same target speed, the measured vehicle speed can vary substantially depending on the soil volume and soil type accumulated at the blade. In addition, disturbances arise from factors such as ground unevenness and slope, variability in compaction state, and left–right imbalance in blade ground reaction forces, which can change the vehicle velocity and turning behavior. Under such conditions, to achieve accurate velocity control, it is necessary to introduce feedback control that takes the measured vehicle velocity as input.

Acknowledgement

This work was supported by Council for Science, Technology and Innovation(CSTI), Cross-ministerial Strategic Innovation Promotion Program (SIP), the 3rd period of SIP “Smart Infrastructure Management System” Grant Number JPJ012187 (Funding agency: Public Works Research Institute).

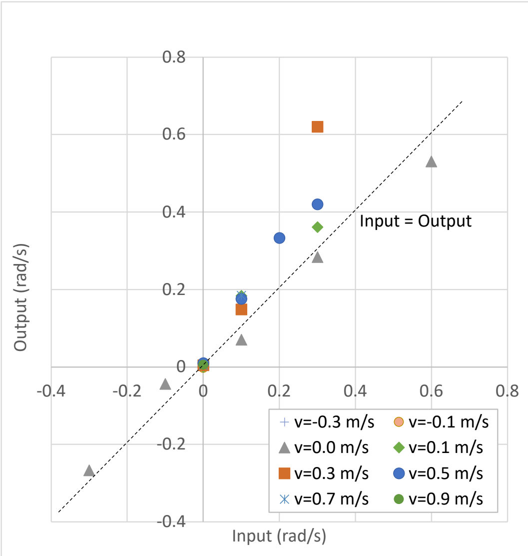

Figure 7. Measured turning velocity for the vehicle velocity input $\boldsymbol{x}$

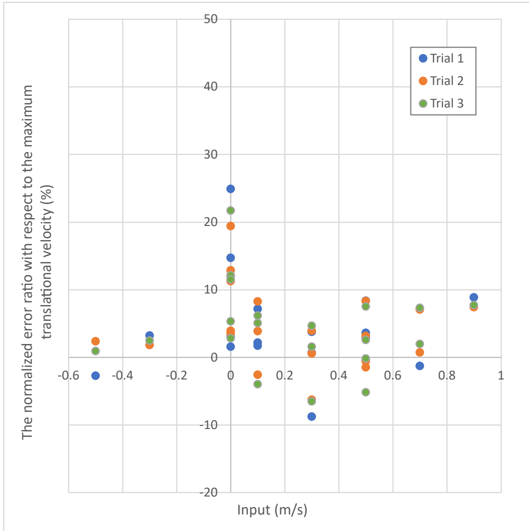

Figure 8. Normalized error ratio of translational velocity with respect to the maximum translational velocity (0.94 m/s) for each input condition over three repeated trials.

References

[1] G. Yamamuchi, D. Endo, H. Suzuki, and T. Hashimoto. Proposal of an open platform for autonomous construction machinery development. In *41th International Symposium on Automation and Robotics in Construction (ISARC 2023)*, 2023.

[2] Christian Frese, Angelika Zube, Philipp Woock, Thomas Emter, Nina Heide, Alexander Albrecht, and Janko Petereit. An autonomous crawler excavator for hazardous environments. *at - Automatisierungstechnik*, 70:859–876, 10 2022. doi:10.1515/auto-2022-0068.

[3] *D37EXi/PXi-24 Crawler Dozer*. Komatsu Europe International N.V., 2016.

[4] *D6K2 Track-Type Tractor: Large Specalog*. Caterpillar, 2014.

[5] Wolfram mathematica. URL `https://www.wolfram.com/mathematica/`.

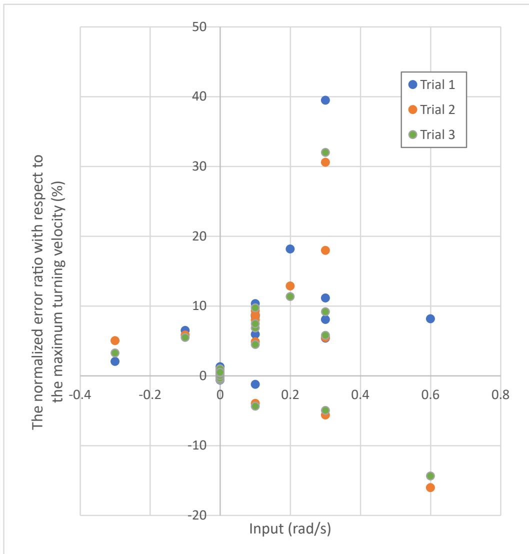

Figure 9. Normalized error ratio of turning velocity with respect to the maximum turning velocity (0.74 rad/s) for each input condition over three repeated trials.